

HYBRID S_N AND RAY-TRACING WITH FICTITIOUS QUADRATURE FOR SIMULATION OF SPECT

Ce Yi and Alireza Haghghat

University of Florida

202 Nuclear Science Building, P.O Box 118300, Gainesville, FL 32611

yice@ufl.edu; haghghat@ufl.edu

ABSTRACT

A hybrid S_N and simplified ray-tracing formulation is developed for simulation of the Single Photon Emission Computational Tomography (SPECT) for a torso phantom. The calculational model can be partitioned into two parts: i) A S_N transport calculation is performed to determine a flux moments distribution in the phantom due to the radioactive source deposited in the heart; ii) A simplified ray-tracing formulation is used to transport particles leaving the phantom surface through a set of collimators normal to the SPECT camera. The Fictitious Quadrature (FQ) technique is developed to integrate the two parts and to evaluate angular fluxes along directions of interest. In this formulation, collimators are not included explicitly. However, their effect is accounted for by using a new circular ordinate splitting technique. We implemented this hybrid formulation in a revision to the TITAN code. The results of the TITAN simulation are in good agreement with the predictions of the reference Monte Carlo SIMIND code. It is also shown that the new hybrid formulation in TITAN results in a higher computational efficiency.

Key Words: TITAN, hybrid, Fictitious Quadrature, SPECT

1. INTRODUCTION

Single Photon Emission Computed Tomography (SPECT) is a nuclear medicine tomographic imaging technique [1]. In SPECT, a small amount of photon radiation source is deposited in the target organ with some nuclear medicine intake. A SPECT gamma camera, rotating around the body, is used to acquire projection images from different angles. The source distribution in the organ can be reconstructed with the projection images. The 3-D source distribution image can be used to diagnose some malfunctions in the organ. Dozens of projection images from different angles are required to reconstruct the source distribution to achieve a good resolution. Collimators are generally used between the camera and the body to filter the gamma rays and allow only the rays along directions close to the normal direction (within a small acceptance angle range) through to reach the camera. In medical physics, SPECT simulation usually is performed with the Monte Carlo approach. In this work, a revision of the TITAN code is used to simulate the projection images of a body phantom.

TITAN is a 3-D hybrid discrete ordinates (S_N) and method of characteristics (MOC) transport code [2]. A block-oriented S_N solver and a block-oriented characteristics solver have been implemented in TITAN. Users can apply either solver in different regions of a problem model. In the SPECT simulation, the revised TITAN uses the S_N formulation in the phantom region, and a simplified ray-tracing formulation in the collimator region. To simulate a projection image

from a certain rotation angle, we use the Fictitious Quadrature (FQ) technique to calculate the boundary angular flux along the rotation angle. Furthermore, since particle absorption and scattering in the collimator region are not simulated in the TITAN model, the circular ordinate splitting technique is developed to account for the collimator blurring effects.

The remainder of this paper is organized as follows. In Section 2, we discuss the hybrid S_N and simplified ray-tracing formulation, including the fictitious quadrature technique and the circular ordinate splitting technique. Numerical results are presented in Section 3. Conclusions are given in Section 4.

2. HYBRID S_N AND SIMPLIFIED RAY-TRACING FORMULATION

The hybrid formulation is comprised of the following steps:

- Step 1 - S_N transport calculation with a regular quadrature set in the phantom region.
- Step 2 - Generation of the fictitious quadrature set with the circular ordinate splitting for a projection angle.
- Step 3 - One extra transport sweep with the fictitious quadrature set in the phantom region using the converged flux moments in Step 1 to evaluate the scattering source for directions in the fictitious quadrature set.
- Step 4 - Simulation of the projections images with the fictitious quadrature set using the simplified ray-tracing formulation in the collimator region.

Note that Steps 2 – 4 are repeated for each projection angle. Step 1 is only required to perform once. We further discuss the steps in the following sections.

2.1. Step 1- S_N Formulation

We use TITAN's S_N solver to perform the transport calculation with a regular quadrature set in the SPECT phantom region. Each voxel of the phantom is modeled as a fine mesh. And we use the 3-D S_N formulation given by [3-4].

$$\begin{aligned}
 & \left(\mu \frac{\partial}{\partial x} + \eta \frac{\partial}{\partial y} + \xi \frac{\partial}{\partial z} \right) \psi_g(x, y, z, \mu, \varphi) + \sigma_g(x, y, z) \psi_g(x, y, z, \mu, \varphi) = \\
 & \sum_{g'=1}^G \sum_{l=0}^L (2l+1) \sigma_{s, g' \rightarrow g, l}(x, y, z) \{ P_l(\mu) \phi_{g', l}(x, y, z) + 2 \sum_{k=1}^l \frac{(l-k)!}{(l+k)!} P_l^k(\mu) \cdot \\
 & [\phi_{C, g', l}^k(x, y, z) \cos(k\varphi) + \phi_{S, g', l}^k(x, y, z) \sin(k\varphi)] \} + \\
 & \frac{\chi_g}{k_o} \sum_{g'=1}^G \nu \sigma_{f, g'}(x, y, z) \phi_{g', 0}(x, y, z) \text{ or } S_g^{\text{fix}}(x, y, z, \mu, \varphi)
 \end{aligned} \tag{1}$$

where,

$\mu, \eta,$ and ξ are the x, y and z direction cosines for the discrete ordinates, (μ, φ) or (μ, η, ξ) specifies a discrete ordinate, where $\mu = \cos(\theta), \eta = \sin(\theta)\cos(\varphi), \xi = \sin(\theta)\sin(\varphi)$. $P_l(\mu) = l$ 'th Legendre polynomial, for $l = 1, 2, \dots, L$, where L is the Legendre expansion order. $P_l^k(\mu) = l$ 'th, k 'th associated Legendre polynomial, and

$\psi_g(x, y, z, \mu, \varphi) =$ Group g angular flux at position (x, y, z) and in direction (μ, φ) within phase space.

$\phi_{g,l} = l$ 'th Legendre scalar flux moment for group g '.

$\phi_{C,g,l}^k(x, y, z) = l$ 'th, k 'th cosine associated Legendre scalar flux moment for group g '.

$\phi_{S,g,l}^k(x, y, z) = l$ 'th, k 'th sine associated Legendre scalar flux moment for group g '.

Other variables in above equations are standard, see Ref. 2 for further detail.

Equation 1 represents the particle balance within a phase space element. The discretized form of Eq. 1 in the Cartesian geometry is expressed by:

$$\frac{\mu_n}{\Delta x}(\psi_{x \text{ out}} - \psi_{x \text{ in}}) + \frac{\eta_n}{\Delta y}(\psi_{y \text{ out}} - \psi_{y \text{ in}}) + \frac{\xi_n}{\Delta z}(\psi_{z \text{ out}} - \psi_{z \text{ in}}) + \sigma_{ijk} \psi_{gijk}^{(n)} = Q_{gijk}^{(n)}, \quad (2)$$

where, $\psi_{gijk}^{(n)}$ is the average angular flux within fine mesh (i, j, k) , for group g and along direction Ω_n . $\Delta x, \Delta y,$ and Δz are the mesh sizes along $x, y,$ and z , respectively, and μ_n, η_n and ξ_n are the direction cosines for discrete direction Ω_n . Subscripts *in* and *out* refer to the incoming and outgoing fluxes, respectively, and $Q_{gijk}^{(n)}$ is the average angular source for the fine mesh as defined by:

$$Q = S_{scattering} + S_{fix} \text{ or } S_{fission}. \quad (3)$$

In Eq. 2 is solved by using a set of auxiliary equations, referred to as the ‘‘differencing’’ scheme. In the SPECT phantom model, we employ the diamond differencing with zero fix-up [3] because of the relatively fine meshing. The Directional Theta-Weighted differencing scheme [5] is also available in the TITAN code.

2.2. Step 2 – Generation of Fictitious Quadrature Set with Circular Ordinate Splitting

To represent the necessary project directions for SPECT imaging, we developed the fictitious quadrature set. This quadrature set include an arbitrary set of directions, which may not be symmetric, and they do not need to conserve the moment of direction consines. Figure 1 shows the directions in a fictitious quadrature set with forty projection angles. Each projection angle has eight split directions.

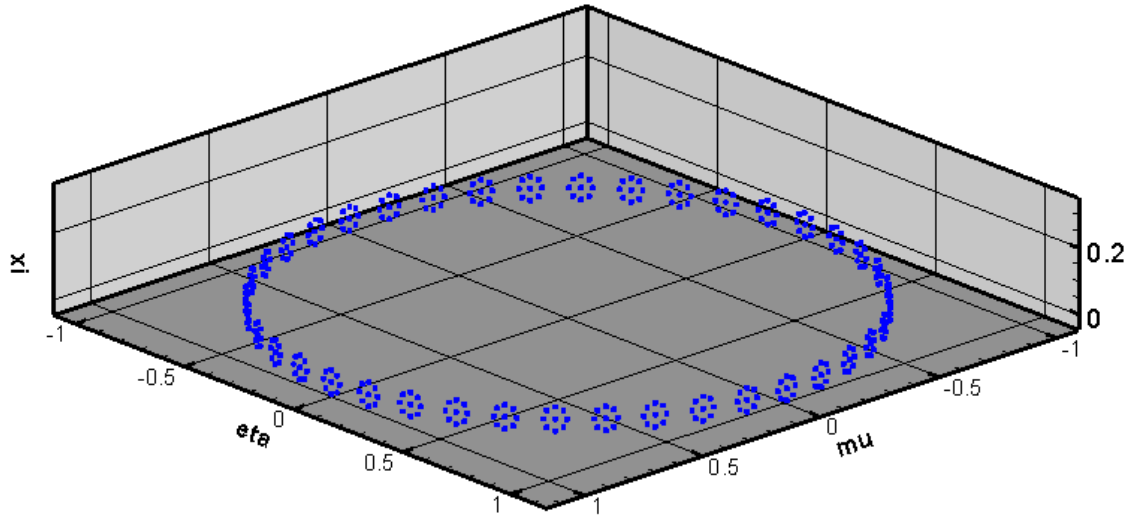


Figure 1. Schematic of a fictitious quadrature set with circular ordinate splitting.

The rectangular and Legendre-Chebyshev Ordinate Splitting techniques [6,7] have been developed to overcome ray effects for problems with highly angular-dependent source and/or angular fluxes. Here, we present the Circular Ordinate Splitting (COS) technique used to simulate the SPECT collimator blurring effect. In the COS, the split directions are located along a circle centered on the original projection direction. The radius of the circle is calculated based on the SPECT collimator acceptance angle. We use quaternions [8] to mathematically describe rotations and calculate the directional cosines for each direction. By averaging the angular fluxes over the original and split directions, we can simulate part of the projection image blurring effects due to the collimator acceptance angle. Note that particle transport within the collimator is not simulated in the deterministic calculation. In other words, we assume all particles travelling outside the acceptance angle will be absorbed in the collimation septa. As with other ordinate splitting techniques, the number of split directions in the COS is determined by the splitting order. The splitting order is the number of directions on one circle, however, a user can consider more than one circle, and therefore achieve a more refined angular representation.

2.3. Step 3 - Extra Transport Sweep with Fictitious Quadrature

A regular angular quadrature set is constructed such that flux moments can be conserved. Fictitious quadrature is designed differently from the regular quadrature type in that its purpose is to calculate only the angular fluxes for certain directions, not to conserve the flux moments. Therefore, it cannot be used in a regular transport sweep, since the scattering source and flux moments cannot be properly handled. However, it can be used to calculate angular fluxes after the source iteration process is completed, i.e., flux moments are converged.

Generally, in a transport problem, users' major concern is the scalar flux distribution and/or *k-eff*. However, in some cases, the angular fluxes in the directions of interest need to be evaluated. Since the directions are not necessarily included in the problem quadrature sets, the angular fluxes in these directions usually cannot directly be calculated by the transport sweep with a regular quadrature set. We have modified the TITAN code for the use of the fictitious quadrature

set. with the modified TITAN allows for an extra transport sweep following the source iteration is converged using a regular quadrature set. The converged flux moments are used to evaluate the scattering source for each direction in the fictitious quadrature by using the following formulation.

$$S_{scattering}^{(e.s.)} = \sum_{g'=1}^G \sum_{l=0}^L (2l+1) \sigma_{s,g' \rightarrow g,l} \left\{ P_l(\mu_n^{(fic)}) \cdot \phi_{g',l}^{(con)} + 2 \sum_{k=1}^l \frac{(l-k)!}{(l+k)!} P_l^k(\mu_n^{(fic)}) \cdot \left[\phi_{C,g',l}^{k,(con)} \cdot \cos(k\varphi_n^{(fic)}) + \phi_{S,g',l}^{k,(con)} \cdot \sin(k\varphi_n^{(fic)}) \right] \right\} \quad (4)$$

Where, superscript (*e.s.*) stands for *extra sweep*, (*fic*) for *fictitious*, (*con*) for *converged*. $\phi_{g',l}^{(con)}$, $\phi_{C,g',l}^{k,(con)}$, and $\phi_{S,g',l}^{k,(con)}$ are the converged ℓ^{th} order *regular*, *cosine* and *sine* flux moments. And $(\mu_n^{(fic)}, \varphi_n^{(fic)})$ specifies a direction in the fictitious quadrature set.

Equation 4 is similar to the scattering kernel used in the regular sweep (Eq. 1), except that we use the converged flux moments after the source iteration process instead of the flux moments from last iteration. The polar and azimuthal angles refer to a direction in the fictitious quadrature set. The fixed source or the fission source can be evaluated in the same way as in a regular sweep process. After the total source is estimated, we can use the extra transport sweep to evaluate angular fluxes for each direction in the fictitious quadrature set.

2.4. Step 4 - Simplified Ray-Tracing Formulation

In the SPECT phantom model, the intensity of each pixel in the projection images is evaluated by the integration of the angular flux at that pixel over the small collimator acceptance angle. We use the simplified ray-tracing formulation to transport particles leaving the phantom surface through a set of collimators normal to the SPECT camera. The simplified formulation assumes particles are travelling through vacuum. Here, we apply the backward ray-tracing approach [5, 6] in TITAN's characteristics solver. The characteristic rays are drawn from each pixel of the projection image backward to the phantom surface along the projection angle and the split directions circularly surrounding it. Each ray will intersect with one of the phantom's four side surfaces. On the phantom surface, the angular fluxes along this projection angle and its split directions are already calculated by the extra sweep with the corresponding fictitious quadrature (Step 3). However, these known angular flux points are located on the centers of fine mesh on the phantom surfaces. Since the ray intersection points are scattered on the surface, a bi-linear interpolation procedure [6] is used to evaluate the angular flux on the intersection points based on the phantom boundary angular flux on the fine mesh centers.

3. NUMERICAL RESULTS

We applied the S_N solver of the TITAN code on a digital heart phantom generated by the NCAT code [9]. NCAT can provide various cardiac-torso phantoms including heart motion. The phantom we used here is the first frame (end-diastole) of the heart motion cycle. The size of the phantom is $40 \times 40 \times 40 \text{ cm}^3$ with $128 \times 128 \times 128$ voxels. The voxel linear size is 0.31 cm.

In the TITAN calculation, we consider the whole phantom as one coarse mesh with 128x128x128 fine meshes (~2 million meshes total), with each fine mesh representing a voxel. A total of five materials are used in this model: air, body (muscle), dry spine bone, dry rib bone, and lung. The material densities are provided in the NCAT attenuation image. The energy range (10 ~ 155 keV) is partitioned into three energy groups. A 3-group cross-section library is generated by the CEPXS code [10]. CEPXS allows the user to define arbitrary group structure. Here the energy group boundaries are 154.55, 126.45, 98.35, and 10 keV. The first energy group (126.45 ~ 154.55 keV) is chosen based on the detector energy resolution for a Tc-99m source (~140 keV). In SPECT, generally only the first group projections are used for reconstruction. Therefore, the other two group boundaries can be chosen arbitrarily. We choose to use the same width for the second group as the first group. In order to include collimator blurring effects in the TITAN model, we integrated the angular flux over the collimator acceptance angle with the circular ordinate splitting technique, and used the averaged angular fluxes on the phantom boundaries to simulate the projection images. Here we tested with different number of projection angles and circular splitting order.

The TITAN results are compared with the SIMIND code [11], a widely used Monte Carlo program for SPECT. When using SIMIND to simulate NCAT phantom, the number of total source particles is the number of voxels with source in the phantom multiplied by a factor (the default value is one). In this phantom, there are about 750,000 voxels with source among the total ~2 million voxels. Therefore, for each projection image, SIMIND uses ~750,000 particles. Figure 2 visually compares the projection images from four angles (anterior, left lateral, posterior, and right lateral) of TITAN and SIMIND.

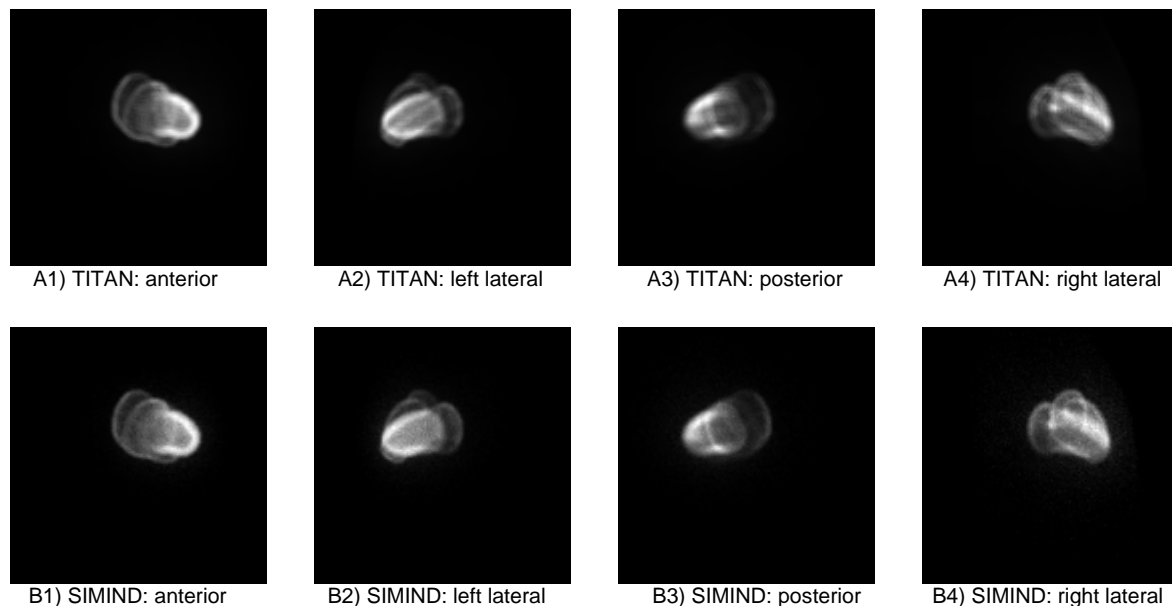


Figure 2. Projections for the first energy bin (126.45 -154.55 keV, images normalized independently).

TITAN computed the lower energy bin projections simultaneously. Figure 3 shows four projections for the third energy group by TITAN.

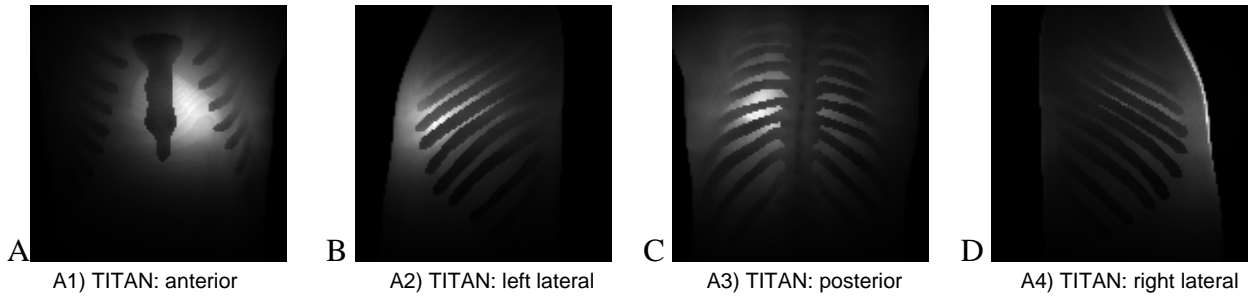


Figure 3. TITAN projections for the third energy bin (10-98 keV, normalized independently).

Table I compares the projections for the first energy bin, quantitatively. Here, we use the infinity norm ($\max\{(C_{\text{titan}}-C_{\text{simind}})/C_{\text{simind}}\}$) to compare the maximum individual pixel difference, and 2-norm to show the overall difference. The 2-norms in Table I are calculated by Eq. 5

$$2 - norm = \frac{1}{N} \sum_{i=1}^N \left(\frac{f_i - r_i}{r_i} \right)^2, \tag{5}$$

Where N is the total number of pixels on one projection image, f_i and r_i are the normalized detector count calculated by TITAN and SIMIND, respectively.

Table I. Relative differences of normalized fluxes obtained by TITAN and SIMIND codes for four imaging projection angles

Error type	Projection angles			
	anterior	left lateral	posterior	Right lateral
Inf-norm	14.52%	21.41%	15.03%	22.30%
2-norm	2.37E-03	3.06E-03	2.73E-03	2.77E-03

The differences could be attributed to the cross section data. TITAN uses the discretized energy group cross-section data generated by CEPXS [10], while the continuous-energy cross section data in SIMIND is tuned to SPECT simulation for body materials. Table II compares the CPU time of SIMIND and TITAN for 4, 60, 120, and 180 projection angles.

Table II. Comparison of CPU times (min) for SIMIND and TITAN codes for different number of imaging projection angles

Method	Number of imaging projection angles			
	4	60	120	180
SIMIND* (min)	7.5	129.2	257.3	390.7
TITAN-SPECT (min)	20.8	27.1	33.8	40.5

Total CPU time for three energy bins ~750,000 particles/projection.

Note that variance reduction techniques are used in the SIMIND code to optimize the evaluation of a single projection at a time. Therefore, SIMIND requires a separate calculation for each projection image for a given energy bin. While SIMIND CPU time is proportional to the number of projection images, the computation cost for TITAN is mostly dedicated to the calculation of the flux moments. After the flux moments are converged, the fictitious quadrature technique is used to compute a projection image with much less cost.

4. CONCLUSIONS

We developed a new hybrid S_N and simplified ray-tracing formulation for the SPECT transport simulation, which usually was performed using the Monte Carlo method before this work. The numerical results show a good agreement with the Monte Carlo reference calculated by the SIMIND code. One advantage of the deterministic method over the Monte Carlo approach is the reduced computation time for simulation of a large number of projection images. Furthermore, in the simulation for lower energy groups, SIMIND usually requires more source particles and scattering tracking. When using SIMIND to simulate the uncollided particle projection images (highest energy bin), generally a particle can be killed after one or two scattering events. For a lower energy bin projection image, SIMIND needs to track more scatterings for a particle to reduce its energy to the desired range, and also requires more source particles to overcome the statistical errors due to lower count. Therefore, it is usually much more expensive for SIMIND to calculate lower energy bin projections. While in the deterministic calculation, the projections for lower energy groups can be calculated the same way as the first energy group with much less additional cost. A convenient feature of TITAN is the support of continuous runs. An initial run of TITAN can dump the flux moments on the hard disk. The following runs can skip the transport simulation step (Step 1 as listed in Section 2) by loading the flux moments from the previous run on the disk, and calculate the projection images for different fictitious quadrature sets. A parallel version of TITAN is also available. It is possible to reduce the simulation time to the clinic requirement.

The fictitious quadrature technique is developed to facilitate the integration of the S_N and simplified ray-tracing formulation. In general, the technique can be used to evaluate the angular flux along directions of interest. It can simulate snapshot “pictures” of the problem model from a number of arbitrary angles by a photon or neutron “camera.” In future studies, the technique could be applied to some reactor shielding simulations.

ACKNOWLEDGMENTS

The authors would like to thank Dr. J. Parker and Dr. D. Gilland from University of Florida, and Dr. M. Ljungberg from Lund University, Sweden, for their kind help in the use of SIMIND code.

REFERENCES

1. E. G. DePuey, E. V. Garcia, and D. S. Berman, *Cardiac SPECT Imaging*, Lippincott Williams & Wilkins, Philadelphia (2001).

2. C. Yi, "Hybrid Discrete Ordinates and Characteristics Method for Solving the Linear Boltzmann Equation," PhD Thesis, University of Florida (2007).
3. B. G. Carlson and K.D. Lathrop, "Discrete Ordinates Angular Quadrature of the Neutron Transport Equation," LA-3186, Los Alamos National Laboratory (1965).
4. E. E. Lewis and W. F. Miller, *Computational Method of Neutron Transport*, John Wiley & Sons, New York (1984).
5. B. Petrovic and A. Haghghat, "New Directional Theta-Weighted S_N Differencing Scheme," *Trans. Am. Nucl. Soc.*, **73**, 195 (1995).
6. C. Yi and A. Haghghat, "A Hybrid Block-Oriented Discrete Ordinates and Characteristics Method Algorithm for Solving Linear Boltzmann Equation" *Proc. Int. Conf. M&C 77* Monterey, CA (2007).
7. G. Logoni and A. Haghghat, "Development of the Regional Angular Refinement and Its Application to the CT-Scan Device," *Trans. Am. Nucl. Soc.*, **86**, 246 (2002).
8. V. Kravchenko, *Applied Quaternionic Analysis*, Heldermann Verlag (2003).
9. W. P. SEGARS, "Development and application of the new dynamic NURBS-based cardiac-torso (NCAT) phantom," PhD Thesis, University of North Carolina (2001).
10. L. J. Lorence, J. E. Morel, and G. D. Valdez, "User's Guide to CEPXS/ONELD: A One-Dimensional Coupled Electron-Photon Discrete Ordinates Code Package," Sandia National Laboratory (1989).
11. M. Ljungberg, S. Strand, and M. King, "The SIMIND Monte Carlo program: Monte Carlo Calculation in Nuclear Medicine," *Applications in Diagnostic Imaging*, **11**, 145 (1998).